

## Effect of surface roughness on the fatigue strength of E-glass composite single lap joint bonded with modified graphene oxide-epoxy adhesive

Ashutosh Manoli , Rohit Ghadge , Parshant Kumar 

MIT World Peace University, Kothrud, Pune, India

✉ [ashu16manoli@gmail.com](mailto:ashu16manoli@gmail.com)

**Abstract.** The inability of manufacturing systems to fabricate near net shape complex structures requires efficient joining techniques for simple components to form a complex structure. Composites adhesive are gaining attention due to their good mechanical properties. The present study aims to improve the mechanical strength of single lap joint of composite material comprises of glass fibers reinforced polymer (GFRP) plates which were joined by nano particles modified adhesive. Epoxy adhesive was modified by dispersing 0.5 wt.% graphene oxide (GO). The surfaces of GFRP plates were prepared for five different surface roughness. The effectiveness of joint was assessed by the enhancement in the fatigue strength and fracture resistance of the single lap joint. The tensile test depicted the peak load of 6.095 kN when the surface roughness was prepared to be 3.316  $\mu\text{m}$ . The observed peak load was 68 % higher as compared to as-prepared composites where the surface roughness was 0.211  $\mu\text{m}$ . Similarly, for the same surface roughness, axial fatigue tests showed 30 % enhancement in number of cycles to failure as compared to as-prepared composites. The results concluded a substantial effect of surface roughness of adherend on the joint strength.

**Keywords:** Cure/Hardening; resin-based composites; Epoxy Resin; Graphene Oxide; Optical Microscopy; Tensile Testing; Fatigue, Scanning Electron Microscopy; Surface Finish; surface treatment.

**Citation:** Manoli A, Ghadge R, Kumar P. Effect of surface roughness on the fatigue strength of E-glass composite single lap joint bonded with modified graphene oxide-epoxy adhesive. *Materials Physics and Mechanics*. 2023;51(2): 65-80. DOI: 10.18149/MPM.5122023\_7.

### Introduction

Fiber-reinforced composites (FRCs) are not new to advanced engineering sectors such as automobiles, aircraft, and shipbuilding industries. However, achieving near-net shapes for big and complex structures is still considered to be difficult. Thus joining methods for FRCs play an important role in depicting their in-service performance. The conventional joining technique like riveting may impose stress concentration effects in the vicinity of the joint. Thus adhesive bonding of FRCs is gaining attention due to its ability to uniformly distribute the stress which thereby relieves the stress concentration effect, and improves the mechanical strength and fatigue resistance [1]. The adhesively bonded joints also lead to weight reduction which increases the specific strength of structures. Despite these advantages, the research on adhesives is not yet fully matured due to various underlying failure mechanisms such as adhesive failure, cohesive failure, fiber-tear failure, stock-break failure, and adhesion promotor failure which are more prominent in one or other. Several researchers [2-5] are designing composite adhesives

to enhance the strength of joint by enhancing strength of adhesive bulk, and strength of substrate/adhesive interface.

In a research work, Korayem et al. [6] modified epoxy adhesive with carbon nanotubes (CNT) to join carbon fiber reinforced polymer (CFRP) composite with steel. It was observed that the effective bond length of CNT-modified epoxy was shorter as compared to pure epoxy adhesive. Thus, the potential of load transfer from steel to CFRP was higher in the case of CNT-modified epoxy adhesive.

In another research work, Saraç et al. [7] observed an increase in static and fatigue strength of epoxy-based adhesive joints when the adhesive was modified with ceramic nanoparticles. The increase in strengths was mainly attributed to the increase in damping capabilities with the addition of nanoparticles. This increased the displacement capacity of the joints which thereby increased the failure loads. Tailoring the composite adhesive by adding different amounts of filler in the matrix is an effective way of increasing the adhesive strength. Moreover, the strength of the substrate/adhesive interface can be tailored by altering the surface characteristics of the substrate.

In a research work, van Dam et al. [8] varied the surface roughness of steel substrates and found that the strength of adhesive joint can be increased with an increase in surface roughness due to mechanical interlocking and an increase in interfacial bond area. However, it may lower the substrate resistance to environmental degradation. Thus, the optimum value of surface roughness is required to improve the in-service performance.

In another research work, L. Guo et al. [9] showed that the parameters like nano-scale pores, wettability, and texture direction also play an important role instead of only surface roughness. The key parameter for composite adhesive is the material system chosen for adhesive. Graphene Oxide (GO) filled epoxy composite had proven its potential as an adhesive. The oxygen-containing functional groups imparts hydrophilic character in GO due to which the interfacial interaction between GO and polar polymer improves significantly [10]. This results in increase in strength of adhesive. Xue et al. [10] observed 56.3 % increase in lap shear strength and 10.2 % increase in Young's modulus with the addition of 1 % Graphene Oxide (GO) in epoxy adhesive. Similarly, Aradhana et al. [11] added GO in epoxy adhesive and observed a 50 % increment in strength with 0.5 wt.% of GO. Thus, GO is an effective reinforcement in an epoxy based adhesive. The present investigation deals with the effect of surface roughness on adhesive characteristics of GO-modified epoxy. Glass fibers reinforced epoxy (GFRP) composites were considered substrates. The adhesive characteristics were assessed by static and fatigue strengths of single lap joints.

S.A. Bansal et al. [12] used the wet chemical oxidation procedure to disperse graphene oxide in an epoxy matrix. The experimentation concluded that the mixture's visco-elastic characteristics had improved noticeably at this point. The study also concluded that 0.5 % GO dispersion resulted in a 10 % increase in the hardness of the epoxy-graphene oxide mixture. To study the tribological characteristics of magnetic iron oxide/graphene oxide ( $\text{Fe}_3\text{O}_4/\text{GO}$ ) nanocomposites under the influence of magnetic fields, A. Sammaiah et al. [13] worked on their synthesis. By increasing the concentration of Graphene Oxide (GO) in nanocomposite under magnetic field, the friction and wear performance was improved by 35.5 %. Aluminum matrix composites loaded with titanium (Ti) particles were employed by C. Rajaganapathy et al. [14] to study the tribological characteristics utilizing a Pin on Disc setup. They claimed that utilizing graphene with titanium reinforcement up to 3 % and 1 % of silver nanoparticles significantly improved the tribological characteristics. Also they found out that if more than 3 % of reinforcement of Graphene and Titanium was made, both the strengths decreased considerably.

M.D. Banea et al. [15] surveyed to analyze composite structures of fiber-reinforced plastics (FRP) that were adhesively bonded. Concerning the adhesive-bonded FRP composite

structure, a brief conclusion was made on the effects of elements such as surface preparation, bonding configuration, adhesion qualities, and environmental variables on bonding conduct.

M.V. Fernandez et al. [16] performed carbon / epoxy composite laminate testing to assess fatigue behavior in load mode I. The main objective here was to obtain a power release rate using various methods of data reduction. Three different data reduction schemes were used in the fatigue characterization of composite bonded joints. The methods allow different ways of calculating the strain energy release rate as a function of crack length, which is a fundamental task to establish a correlation with fatigue crack growth rate. The results obtained demonstrated that this method provides results that are consistent with the ones provided by the classical beam theory method. Some non-negligible differences were obtained relative to the compliance calibration method, which was attributed to the difficulties of the third-polynomial adjustment to the compliance versus crack length.

The research by J. Wei et al. [17] focuses on the different processing techniques for nanocomposites as well as their mechanical, electrical, and thermal characteristics. The study discovered that insufficient mixing resulted in lumps and uneven dispersion, which reduced the mechanical and thermal performance of nanocomposite materials. Carbon nanotubes (CNTs), nano clay, nano silica (nano-SiO<sub>2</sub>), graphene nanoplatelets (GNPs), and nano alumina were among the nanofillers examined by P. Jojibabu et al. [18] (nano-Al<sub>2</sub>O<sub>3</sub>). According to the literature, the type of Nano filler dispersed in the epoxy can increase binding strength by up to 70%. Also, it was found out that the Nano particles that were spherical in shape were lesser effective when compared to the Nano particles with flat or plate like morphology.

Rohit R Ghadge et al. [19] conducted experimentation on various wt.% of graphene oxide dispersed in epoxy resin. A maximum of 33 % improvement in fracture toughness was reported with the dispersion of 0.25 wt.% graphene oxide. Also, significant improvement in fatigue cycles was observed in with the addition of graphene oxide compared to neat epoxy.

S. Budhe et al. [20] investigated the impact of adherend surface roughness on adhesive fatigue life. Surface roughness and adhesive bond strength were shown to be correlated. For aluminum and wood adherend joints, respectively, optimal surface roughness values were found to be in the range of  $Ra = 1.68 \pm 0.14 \mu m$  and  $Ra = 1.64 \pm 0.2 \mu m$ .

P. Jojibabu et al. [21] demonstrated high epoxy-based adhesion of graphene nanoplatelets (GNPs) and triblock copolymers (BCPs) divided into phases to improve the strength of lap shear joints adhesive aluminum sheets. It was noted that the addition of 1wt.% of OZ-GNPs to about 10 wt.% SBM-modified epoxy adhesive resulted in a lap shear strength increase of 129%, compared to unchanged epoxy resin.

P. Upadhyaya et al. [22] used a method based on simulation. They used the atomistic-based modeling (ABC) model method and found a 30 % improvement in Single lap joint strength using 2 % concentrated CNT. In order to create/form graphene nanocomposites, M.A. Rafiee et al. [23] investigated and evaluated the characteristics of graphene and Functionalized Graphene Sheets (FGS). In this study, 0.125 wt.% FGS nanocomposites were found to improve fracture toughness by about 65% and fracture energy by about 115 %. Several studies [24] have been conducted to verify the strength parameters of each lap joint, with the addition of silica nanoparticles and multi-walled carbon nanotubes increasing average shear strength and fracture point elongation by 28 % and 36 %, respectively.

B. Soltannia et al. [25] investigated the effect of Nano-reinforcing materials on the mechanical response of single-wrap joints bonded with composite adhesives exposed to various strain rates. Impact test results show the positive effect of Nano-reinforcing on the stress sensitivity of the joint by increasing the stiffness and strength of the joint overall.

M.M. Shokreih et al. [26] investigated the impact of adding a mixture of carbon nanofibers (CNFs) and graphene nanosheets (GNFs) on the flexural fatigue behaviour of epoxy polymer. Based on shifting magnetic fields, graphene nanosheets were created. The samples

were subjected to various fatigue loadings with varying displacement amplitudes. Hybrid nanoparticle addition resulted in a notable improvement in the fatigue life of epoxy resin. Experimental results showed that adding 0.5 weight percent of hybrid nanoparticles increased strength ratio by 43 %, but adding graphene and CNF increased strength ratio by only 27.4 and 24 %, respectively.

The examination of the mechanical properties of E-glass fiber reinforced polymer nanocomposites was conducted by B.V. Kiran et al. [27] where graphene oxide nano platelets (GONP) based polymer nanocomposite material with E-glass fiber reinforcement was made utilizing the hand layup technique. graphene oxide nano platelets (GONP) based polymer nanocomposite material with E-Glass fiber reinforcement was made utilizing the hand layup technique. The author added four concentrations of nano particles in epoxy resin (0.5, 1, 1.5 and 2 wt.%). In addition to SEM testing, several tests were carried out, including tension, compression, hardness, toughness, and flexural tests. It was discovered through experimental research that the material's tensile strength and compressive strength had grown, with percentages of 10.25, 14.97, 16.26, 18.64, and 1.97, 3.46, 5.65, and 11.56 correspondingly. In addition to increasing the tensile and compressive strengths, the flexural strength increased by percentages of 4, 19.92, 26.78, and 28.73, respectively.

Improvements in fatigue life and fracture toughness in graphene oxide/epoxy composites were researched by D.R. Bortz et al. [28]. Uniquely, open helical-ribbon carbon nanofibers were unraveled and splayed to create graphene oxide. report improvements of up to 15-80% in uniaxial tensile fatigue life and 28-111 % in mode I fracture toughness by adding tiny amounts (less than 1 weight percent) of graphene oxide to an epoxy system. Only 0.1 weight percent of graphene oxide added resulted in a 12 % increase in tensile modulus. Flexural stiffness and strength were respectively 12 and 23 % higher at 1 wt.% compared to the unaltered epoxy.

S. Jahandideh et al. [29] studied the effect of different concentrations of graphene oxide on the mechanical properties and flexural strength of composite. It was found out that the addition of more than 0.5wt% of GO in epoxy resin causes agglomeration of GO particles and decrease the flexural strength and flexural modulus of the composite.

## Material and Methods

**Materials.** The materials used for the experimentation were E-glass composite, epoxy resin Epofine 740, epoxy hardener Finehard 918, epoxy hardener accelerator 062 and graphene oxide nano powder. The epoxy resin, epoxy hardener and hardener accelerator were supplied by Fine Finish Organics Pvt. Ltd. and graphene oxide powder by Ad-nano Technologies Pvt Ltd. The properties of graphene oxide powder are as shown in the Table 1.

**Table 1.** Properties of graphene oxide

Graphene Oxide	Description
Purity	~99%
Thickness	~0.8-2 mm
Dimension	~5-10 $\mu\text{m}$
Layers	1-3
Carbon Content	~60-80%
Oxygen Content	~15-32%
Surface Area	110-250* $\text{m}^2/\text{g}$
Bulk Density	0.5 $\text{g}/\text{cm}^3$
Physical form	Fluffy, very light powder
Odour	Odourless
Colour	Black

**Table 2.** Properties of Epoxy hardener and Hardener accelerator

Sr. No	Description	Unit	Specification	Measured value	Test method
<b>Epoxy Hardener Finehard 918</b>					
1	Color	-	Colorless-Pale yellow	Colorless	Visual
2	Clarity	-	Clear liquid	Clear liquid	Visual
3	Viscosity@25°C	mPa s	40 - 70	56.74	ASTM D 2196-18
4	Specific Gravity at 25 °C	-	1.14 – 1.20	1.153	IS 9162-1979
<b>Epoxy Hardener Accelerator 062</b>					
5	Color	-	Colorless	Colorless	Visual
6	Clarity	-	Clear Liquid	Clear	Visual
7	Density at 25 °C	g/ml	0.88 - 0.92	0.8944	IS 101 (part 1/Sec 7) - 1987

**Methods.** The use of composite materials in industries has started increasing due to their enhanced mechanical and fatigue properties. Hence, the need to study various bonding materials for the composite materials also plays a lot of importance. This has opened the possibility of the use of Nanomaterials in adhesives to increase their tensile as well as fatigue properties. E-glass composite material was used as an adhered in this research. The E-glass/epoxy composite orientation used in the Experimental Analysis was [0/45/-45/90]s. The dimension of the E-glass slab is taken as 100×25 ×3 mm according to ASTM D5868 standards. The adhesive thickness was restricted to 0.74mm as per ASTM D5868 standards. (Figure 2(d)).

Many researchers have been working on the dispersion of nanocomposites such as graphene Nano palettes (GNPs) and carbon nanotubes (CNTs). but there is very limited research on the dispersion of Graphene Oxide (GO) nanomaterial in epoxy resin for adhesive preparation. Hence, this research focuses on the adhesive using the dispersion of GO Nano material into epoxy resin. 0.5 wt.% GO was dispersed in epoxy resin for the adhesive preparation. 5 different surface roughness of the adhered were obtained by the use of different grades of sandpapers, emery papers, and laser cutting machine.

**Preparation of SLJ.** 500 g/m<sup>2</sup> HinFabTM HGU500 fiberglass and epoxy matrix were selected as the composite material. The fiber orientation in the laminate was chosen to be [0/45/-45/90] s. This symmetric configuration was chosen to provide and increase ultimate strength in all directions of the laminate. Laminates were created using the hand lay-up method and 100×25×3 mm panels were used to create single wrap joints. After the matrix became sticky, it was press-cured in an oven at 70 °C for 3 hours and then cooled to normal room temperature. Surface preparation of specimens was done using different grits of sandpaper, emery paper, and a laser cutting machine. The area of bonding measuring 25×25 mm was surface finished obtaining different roughness values (measured in R<sub>a</sub>). Five different surface roughness were obtained on the adhered surface with the parameters shown in the table below (Table 3). The laser cutting machine was used to obtain higher surface roughness as it was not possible to use sand papers.

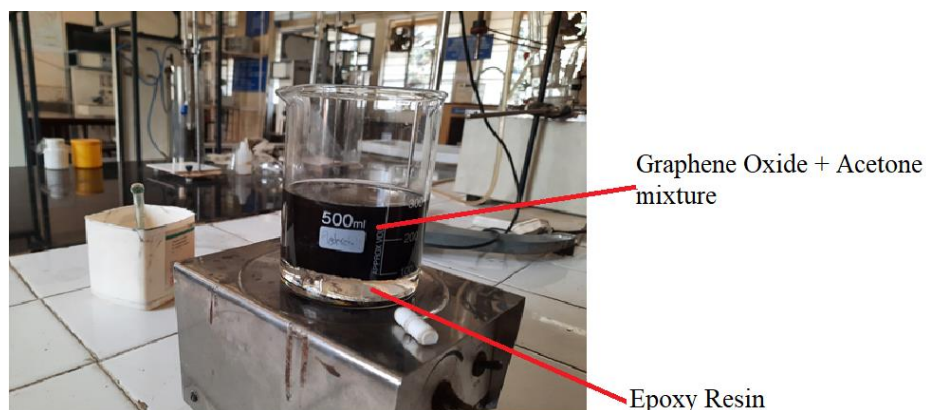
**Table 3.** Machine and sand paper parameters

Sr no	Grit	Speed, mm/s	Power, W	Interval,	Roughness (Ra) Avg, $\mu\text{m}$
NO SURFACE TREATMENT					
1	-	-	-	-	0.211
SAND PAPER					
2	G80	-	-	-	1.7712
3	G36	-	-	-	3.3168
LASER CUTTING MACHINE					
4	-	200	10	25	4.128
5	-	175	15	35	9.01

The parameters for the laser cutting machine were finalized by the trial-and-error process to get the desired surface roughness value of the adhered. First, random parameters were set on the laser cutting machine and the surface roughness obtained on the specimen was observed. If the desired surface roughness was obtained as shown in table 3, then the respective machining parameters were finalized.

**Adhesive Preparation.** 0.5 wt.% graphene oxide-epoxy resin adhesive was selected for the study. This is because the study [29] showed that using GO concentrations higher than 0.5 wt% caused agglomeration of graphene oxide in the epoxy matrix further leading to decrease in the flexural strength and flexural modulus.

During the preparation of the GO-Epoxy adhesive, the dispersion of the Graphene oxide nano particles in epoxy resin plays an important role. The graphene oxide particles have to be evenly dispersed in the epoxy resin so as to get uniform properties of the adhesive on curing. Care must be taken that there is no agglomeration/lump of the graphene oxide particles in the resin to avoid non uniform bonding properties of the adhesive. Here, acetone was used to initially disperse the graphene oxide uniformly in it. Acetone was selected because it has low boiling temperature of approximately 40 °C. This helps in the later evaporation part of the acetone is highly volatile in nature.

**Fig. 1.** Prepared mixture of epoxy resin and graphene oxide

Here, first the measured quantity graphene oxide (0.5 gm) was mixed in acetone. The dispersion was done in the concentration of 2 mg/ml of acetone. This mixture was then kept in ultrasonic bath for 2 h. for allowing proper dispersion of graphene oxide in acetone. Now, this entire mixture was poured in a beaker which had measured quantity of Epoxy resin (100 gm). This mixture was then kept on the magnetic stirrer for 4.5 to 5 hours (Fig. 1). Initially the

acetone in the mixture makes the resin lose its viscosity. But the epoxy resin regains its viscosity due to evaporation of acetone. Again, the mixture was kept in heated water bath till acetone was completely evaporated. Thus, a well dispersed GO-epoxy composite adhesive was prepared by mixing the epoxy resin, hardener and accelerator in the ratio of 100:90:1.

**Design of wooden Fixture.** According to ASTM D5868 standards, the thickness of the adhesives should be kept around 0.76 mm during the lap joint preparation. This causes the need for a fixture that separates the two plates by a distance of 0.76 mm during the lap joint preparation. Hence, to maintain this thickness, a simple wooden fixture was designed. It was designed by the use of plywood for the base and 4mm ply which was surface treated to reduce its thickness to around 3.28 mm. This thin plywood was then glued to the base plywood to form a complete structure. This made it possible for maintaining the specified adhesive thickness according to ASTM standards. (Fig. 2(a,b)).

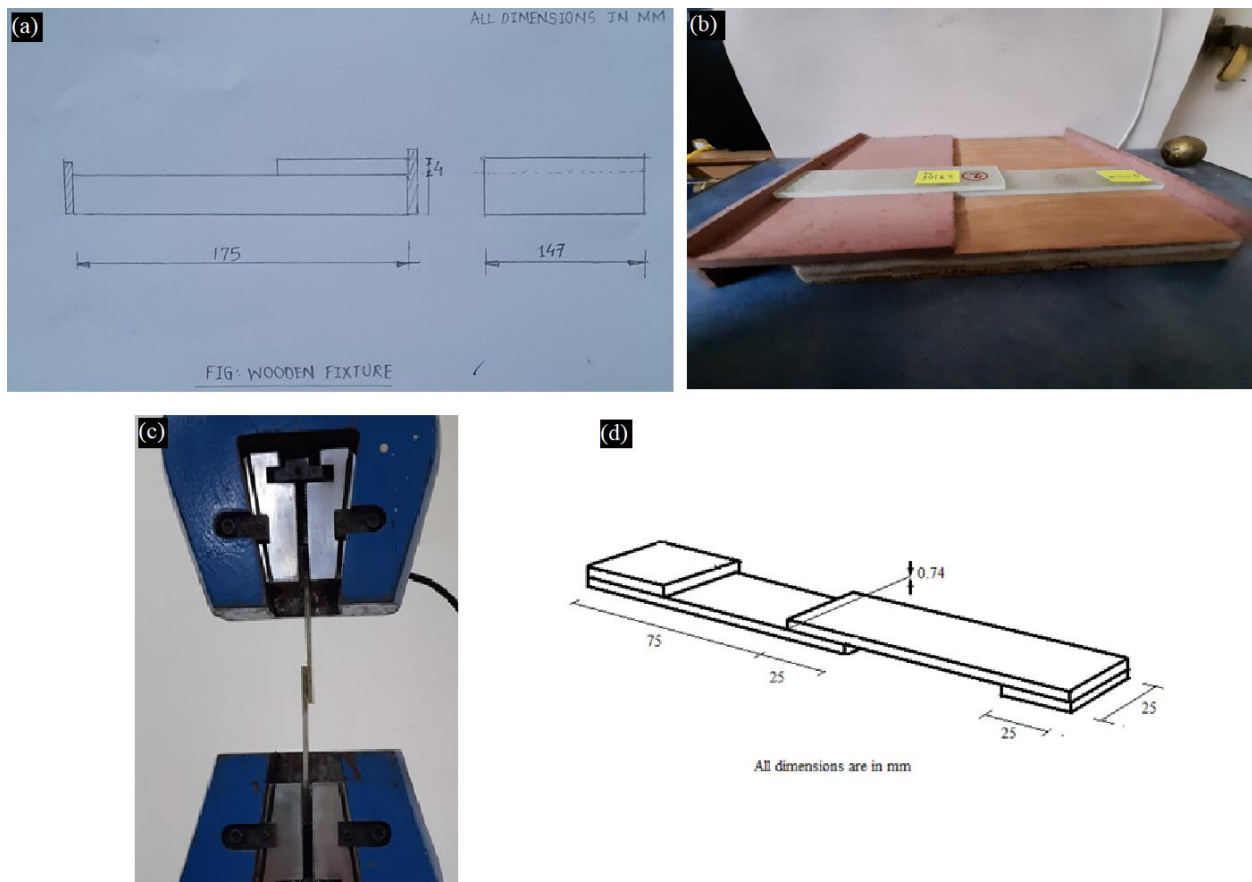


**Fig. 2.** (a) Fixture sketch, (b) Actual fixture, (c) Clamped specimen, (d) Specimen dimensions

The dispersion of the graphene oxide in epoxy resin plays an important role in the final adhesive quality. Hence, to ensure this, a sample drop of the prepared adhesive was taken on a slide and observed under an optical microscope at 100x magnification.



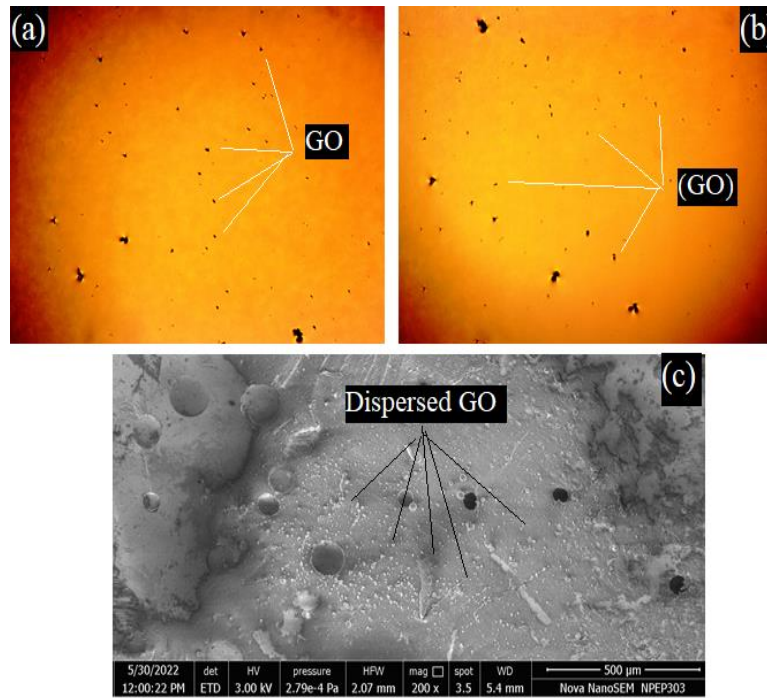


**Fig. 3.** (a) 0.5 wt% GO (Graphene Oxide) dispersion in epoxy resin taken at 2 different positions at 100x magnification, (b) SEM image of dispersion at 200x

Images were taken at 2 different spots on the prepared adhesive. As seen from the optical microscopic images in Fig. 3(a,b), it was observed that the graphene oxide dispersion was uniform throughout the epoxy resin with no visible agglomeration/lump formation of graphene oxide. Three images were captured at two different positions of the adhesive drop taken on a slide. The black spots represent the graphene oxide nanoparticles dispersed in the epoxy resin (orange in color for better visibility). Figure 3(c) shows the dispersed graphene oxide (GO) particles. The dispersed GO particles are visible as white spots as seen in the image. After this, the adhesive was ready for application on the E-glass plates to prepare single lap joints. Now, the hardener and the hardener accelerator were added to the prepared adhesive followed by further curing. The epoxy resin, hardener, and accelerator were mixed in a ratio of 100:90:1. After the addition of the hardener and accelerator, the mixture was stirred to ensure proper mixing of all three. Now the adhesive was ready for application on the adhered.

The prepared GO-Epoxy resin adhesive was applied on the adhered material. The adhered was placed on the prepared fixture as shown in the Fig. 2(b) to maintain the thickness of the adhesive (0.76 mm) as per ASTM D5868 standard. Care was taken to avoid slippage of specimens. The setup was kept undisturbed till the adhesive became tacky. After the adhesive was visibly tacky, the whole setup was taken for the curing process. After the application of the adhesive on the adhered, it was allowed to become tacky. After becoming tacky, it was cured in a hot air oven. For curing, the adhered was placed in the hot air oven at a temperature of 120 °C for 120 minutes. After the curing process, the single lap joints were kept at room temperature for cooling. The prepared samples were ready for tensile and fatigue testing.



**Results and Discussion**

Tensile testing and fatigue testing was performed on the ready specimens to calculate the tensile shear strength and fatigue life of the adhesive bond of the specimens.

**Tensile testing of specimens.** It was necessary to conduct tensile testing to observe the maximum peak load, yield stress, and tensile shear strength of the bonded joint. The tensile testing of the specimen was carried out with reference to ASTM D5848 standards. Testing was done on UTM of 100 KN capacity. The crosshead travel was set to 3 mm/min. An average of 3 specimens was recorded for better accuracy. The specimen was held rigidly in C clamps at both ends and care was taken to avoid any kind of slippage. The tensile testing was carried out until the debonding of the specimen took place. The graphs for load vs displacement were captured and recorded. The maximum load before debonding was also recorded for all the specimens (Table 4). As seen in Fig. 2(c), the test was stopped after the debonding of the specimen took place and the corresponding maximum peak load and stress were noted. It was observed that as the surface roughness increases, the maximum peak load that can be sustained by lap joint before debonding also increases. Figure 4 shows the comparison graph for max peak load of all 5 specimens. Specimen 1 with roughness value of 0.211  $\mu\text{m}$  was used as base value for comparison. The maximum value of peak load sustained of 6.095 KN, and tensile strength of 81.267  $\text{N}/\text{mm}^2$  was observed at a roughness value of 3.316  $\mu\text{m}$  (sample 3). But as the roughness value increases beyond 3.316  $\mu\text{m}$ , the maximum peak load sustained by the lap joint before debonding starts decreasing. Finally for over 9 microns roughness, the maximum peak load reduced to 4.705 KN, further reducing the tensile strength to 62.733  $\text{N}/\text{mm}^2$ .

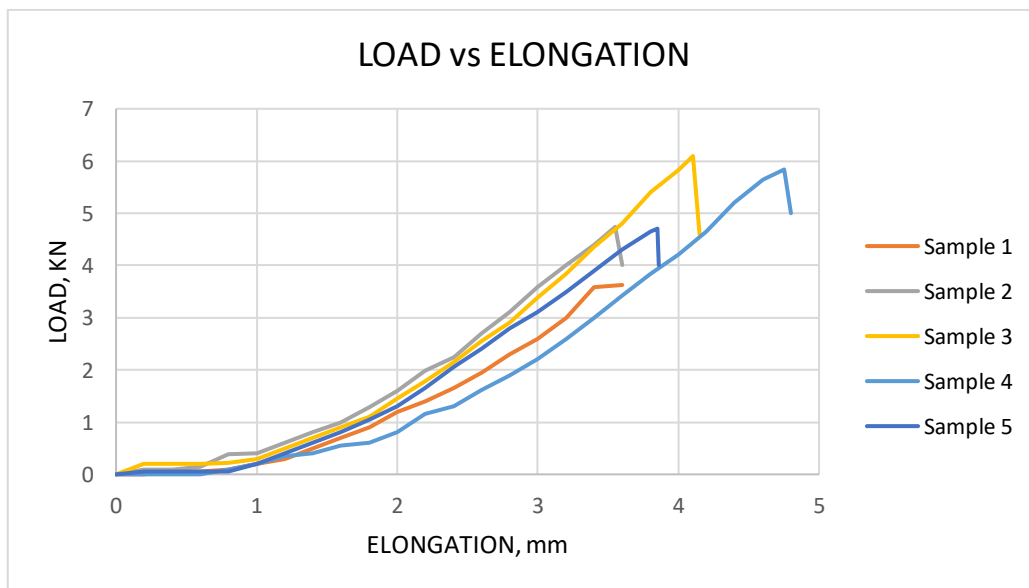


**Fig. 4.** Load vs Displacement graph for specimens

**Table 4.** Max peak load, yield stress and tensile strength

Sample No.	Surface roughness ( $R_a$ ), $\mu\text{m}$	Avg. Max Peak Load, KN	Avg. Yield Stress, $\text{N}/\text{mm}^2$	Avg. Tensile shear Strength, $\text{N}/\text{mm}^2$
1	0.211	3.626	38.587	48.347
2	1.771	4.738	50.533	63.173
3	3.316	6.095	64.813	81.267
4	4.128	5.838	62.2	77.840
5	9.045	4.705	50.187	62.733

The trend in the results obtained followed a similar trend as observed by S. Budhe et. al. [20] where an increase in the mechanical properties was seen with the increase in surface roughness up to an optimal surface roughness after which the reduction in properties is observed. As seen in Fig. 4, the increase in maximum load took place due to an increase in bond strength of the adhesive due to the surface roughness of the bonding area. The results of the tensile testing were tabulated as shown above (Table 4). The values were calculated by the Universal Testing Machine (UTM) and displayed on the interface screen.

**Fatigue testing of specimens.** It was necessary to conduct the fatigue tests on the specimens so as to observe any changes in the bond strength by observing the fatigue life (maximum number of cycles sustained before debonding) for different surface roughness of the specimens. The results were not compared with neat epoxy because the main aim was to study the effect of surface roughness on bond strength and not the effect of different concentrations of graphene oxide in epoxy resin which is already done by other researchers.

The fatigue testing was carried out on the computerized axial fatigue testing machine of 50 KN capacity according to ASTM D5868 standards. Specimen 1 with roughness value of 0.211  $\mu\text{m}$  was used as base value for comparison. The specimens were initially loaded at 50 % of its ultimate load bearing capacity and gradually increased up to 90 % to avoid sudden jerking and failure of material. The frequency was set to 3 Hz. 3 samples of each specimen were tested and average of the three was taken for better accuracy. Initially, the first specimen ( $R_a = 0.211 \mu\text{m}$ ) sustained an average of 14680 cycles before failure due to shear. (Table 5)

Maximum number of cycles observed during fatigue testing was 19,147 for Sample 3 with  $R_a = 3.316 \mu\text{m}$ . The results of the fatigue testing are concluded in the table below (Table 5).

**Table 5.** Fatigue testing results

Sample No.	a Number of cycles	b Number of cycles	c Number of cycles	Avg Number of cycles	Roughness value $R_a$ , $\mu\text{m}$	Max. peak load sustained in tensile testing, KN	50 % of load, KN	90 % of load, KN
1	14461	14900	14500	14620	0.211	3.626	1.813	3.263
2	16100	16152	16250	16167	1.771	4.738	2.369	3.263
3	19146	18637	19658	19147	3.316	6.095	3.047	5.485
4	15214	15525	15350	15363	4.128	5.838	2.919	5.254
5	12957	13275	13316	13182	9.045	4.705	2.352	4.234

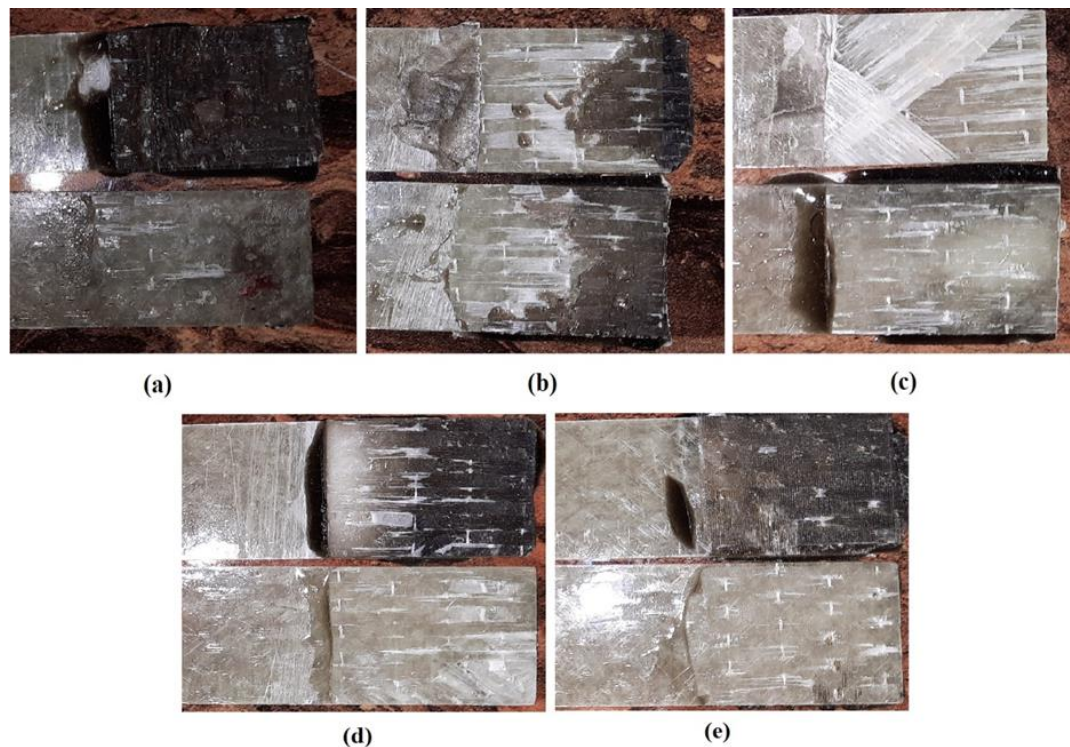
It was observed in the fatigue testing that the maximum bond strength was observed for sample 3 with surface roughness 3.316  $\mu\text{m}$  as it sustained 19147 cycles before fatigue failure indicating maximum bond strength. Sample 1 sustained an average of 14260 cycles, which increased to 16167 cycles for sample 2 and the minimum cycles were observed for sample 5 with surface roughness 9.045  $\mu\text{m}$ , thus showcasing the least bond strength. These results obtained were compared with results obtained by research conducted by R.R Ghadge et al. [19].

Table 6 shows the result table obtained in [19]. There was no adhered surface modification done in this research by the author. The adhesive that was used by the author in the research was similar to the one used in this research. Also, the orientation of the E glass fibers was also similar to the one used in this research i.e. [0/45/-45/90] s. Comparing Table 5 and Table 6, it was seen that almost similar fatigue life (3.8 % less) was obtained for lower GO/Epoxy concentration of 0.5 wt.% as compared to 0.75 wt.% in Table 6. This was made possible by only increasing the surface roughness to 3.316  $\mu\text{m}$ , thus indicating an increase in bond strength resulting an increase in fatigue life due to change in surface roughness of the specimen.

**Table 6.** Fatigue testing results in other literature [19]

Sr. No	Specimen type	Sample no	90 % load, KN	No. of cycles to failure	Average no. of cycles to failure
1	0.75% wt. GO/Epoxy	1	3.046	19752	19904
		2	3.046	20970	
		3	3.046	18549	
		4	3.046	19577	
		5	3.046	20672	

Cohesive failures along with the mechanical interlocking phenomenon are the possible explanation for the variation in bonding shear strength due to change in surface roughness of adhered.

**Fig. 5.** De-bonded specimens:

(a) Sample 1, (b) Sample 2, (c) Sample 3, (d) Sample 4, (e) Sample 5

Figure 5 shows the de-bonded specimen images of different specimens. Initial observation of the de-bonded specimens was made by naked eyes. Figure 5(a) shows the de-bonded specimen with a surface roughness of  $0.211 \mu\text{m}$  and 5(b) with surface roughness. Sample 1, sample 4, and sample 5, (Fig. 5 (a,d,e)) were seen to have undergone adhesive failure. This was because the debonding occurred in the specimen leaving the complete layer of adhesive on one of the surfaces of the adhered as the adhesive can be seen on only one adhered. Sample 2 (Figure 5(b)) underwent cohesive failure. This was because the debonding occurred in the specimen causing the adhesive layer to break from the center leaving the adhesive layer on both the surfaces of the adhered. Sample 3 (Fig. 5(c)) showed substrate failure. This is because the debonding occurred in the specimen causing a complete failure of the fibers of the surface. This type of failure is indicating the possibility of higher bond strength of the adhesive compared to the mechanical strength of the substrate. The increase in surface roughness of the adhered increases the total area of the adhesive joint. The statistics clearly show that roughness

has a significant impact on adhesion and that there is a correlation between both roughness parameters and shear strength. The abraded surfaces were discovered to have a harsh, scratchy surface texture from the microscopic study. These surface features don't interlock, but they do offer a bigger surface area for bonding with the adhesive and the potential for the glue to flow into the scratches. The fact that the average roughness and developed interfacial area follow a similar pattern indicates that the increased adhesion caused by mechanical abrasion can be mostly attributable to the increased surface area induced by the roughening and not to the mechanical interlocking of surfaces.

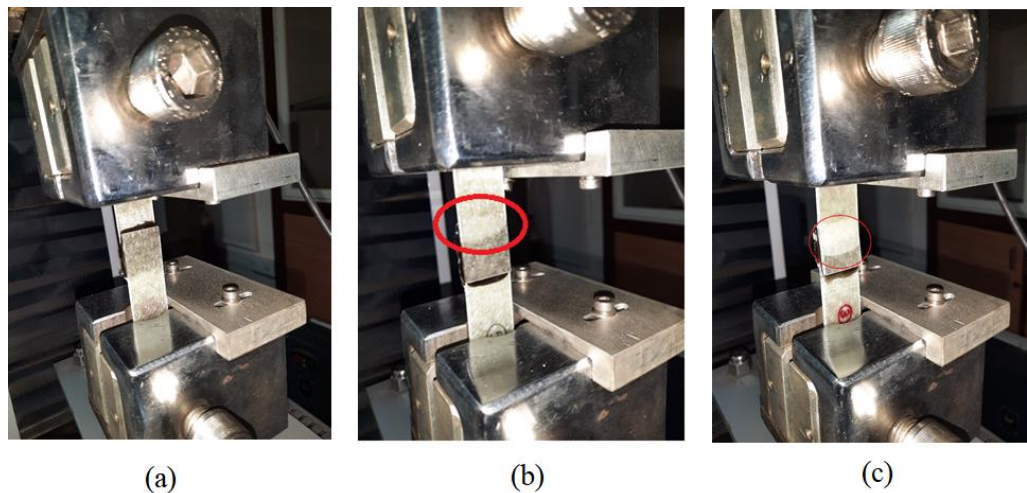


**Fig. 6.** Delamination pattern of specimen

The delamination of specimens occurred as shown in Figure 6. Figure 6(a) shows us the initial specimen at the start of the fatigue test. We can see that the specimen is completely bonded. Later, during the testing, the delamination of the specimen slowly starts as shown in Fig. 6(b). The start of delamination was easily noticed and indicated by a red circle on the specimen. It can be observed that delamination started from the top and started to progress in the downward direction. This is because the shear force acting on the adhesive layer causes initiation of crack and propagates throughout the layer to further cause complete delamination of the specimen (Fig. 6(c)). The debonding may have occurred due to crack propagation.

**Scanning Electron Microscopy of tested specimens.** According to the ASTM D5573-99 standards, there are total seven failure modes of fiber reinforced plastics bonded joints. Scanning electron microscopy (SEM) was performed on fatigue tested specimens to investigate the failure mode of the de-bonded specimens. Mode of failure can only be understood by analyzing the surface of failed specimen. The area of overlap was of interest. A  $5 \times 5 \times 3$  mm sample of the respective specimens was cut for SEM. The material initially is non-conducting. Hence, it is sputtered with gold to make it conducting. Following were the SEM images obtained for 5 different samples of the tested specimens (Fig. 7).



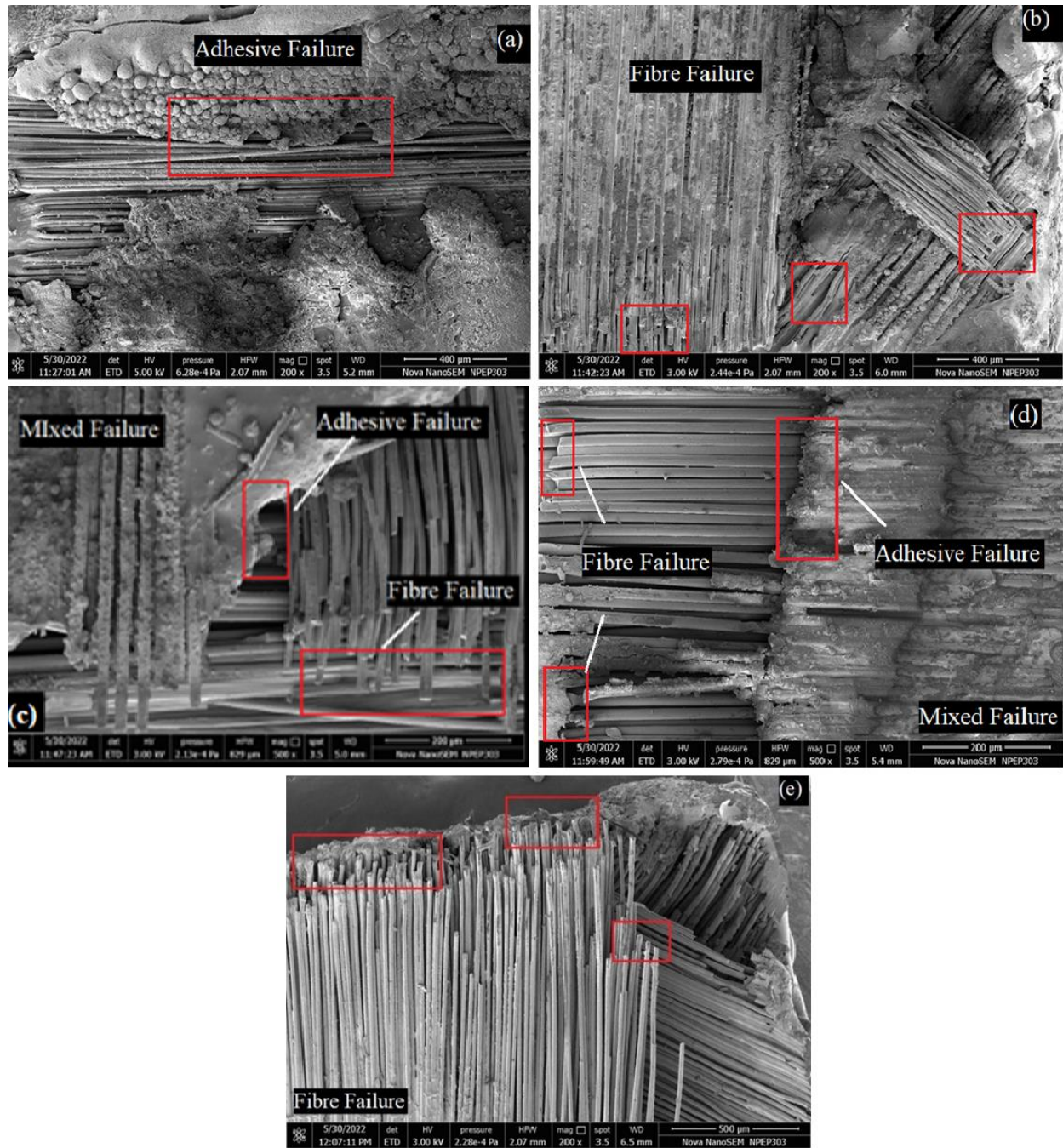


**Fig. 7.** SEM surface images for different surface roughness: (a) Sample 1 ( $R_a = 0.211 \mu\text{m}$ ), (b) Sample 2 ( $R_a = 1.771 \mu\text{m}$ ), (c) Sample 3 ( $R_a = 3.316 \mu\text{m}$ ), (d) Sample 4 ( $R_a = 4.128 \mu\text{m}$ ), (e) Sample 5 ( $R_a = 9.045 \mu\text{m}$ )

Figure 7(a) shows that the complete breaking of adhesive layer due to shear force during fatigue testing. Hence, it concluded that sample 1 has failed due to adhesive failure wherein only adhesive is seen to be failed keeping the below fibers intact. The shear forces generated during the fatigue testing caused the crack propagation only through the adhesive layer. Figure 7(b) and Fig. 7(e) (sample 2 and sample 5) showed fiber failure as the fiber layers below the adhesive have completely failed. This may be possible due to increased bond strength, changing the direction of crack propagation and damaging the fibers below the adhesive layer. In Fig. 7(c) (sample 3), it was observed that both the adhesive layer and fibers have failed due to the shear

force on the specimen. Hence, Fig. 6(c) shows mixed type of failure. Figure 7(d) (sample 4) showed mixed type of failure wherein both adhesive and fibers are seen to be failed.

### Conclusion

The dispersion of GO (graphene oxide) nano particles in epoxy adhesive causes deviation in the crack growth path to a notified different longer path. This is because of GO's unique ability to fill in the small micro cracks that may occur within the material during the loading conditions. Due to this, the final failure of the material is slowed down and ultimately, it improves the mechanical characteristics of the material. Also, the increase in surface roughness of the bonding area increases the surface area available for the GO particles and thus increases the mechanical properties up to a limit. Increasing the surface roughness of the bonding area beyond this limit causes agglomeration of the GO particles which causes reduction in the mechanical properties of the material.

The surfaces of GFRP adhered were prepared for different surface roughness. A graphene oxide filled epoxy material system was used as adhesive. A significant effect of surface roughness on the joint strength was observed. It was noticed that surface roughness of the contact area of the adhered for the adhesive enhances the tensile and fatigue properties of the bond. The tensile and fatigue testing of the specimens showed a noticeable variation in the tensile strength and fatigue life of the specimens. Maximum sustained peak load observed during tensile testing was 6.095 KN for Sample 3 with  $R_a = 3.316 \mu\text{m}$  which was an enhancement of 68% over 3.626 KN for Sample 1 with  $R_a = 0.211 \mu\text{m}$ . Maximum tensile strength observed during tensile testing was  $81.267 \text{ N/mm}^2$  for Sample 3 with  $R_a = 3.316 \mu\text{m}$  which was an enhancement of 68 % over  $48.347 \text{ N/mm}^2$  for Sample 1 with  $R_a = 0.211 \mu\text{m}$ . Maximum number of cycles observed during fatigue testing was 19,147 for Sample 3 with  $R_a = 3.316 \mu\text{m}$  which was an enhancement of 30 % over 14,620 cycles for Sample 1 with  $R_a = 0.211 \mu\text{m}$ , thus indicating maximum bond strength. Increase in both the fatigue and tensile strength with the same amount of GO (0.5 wt.%) in the epoxy adhesive indicated the major outcome that increase in surface roughness increases the fatigue and tensile strength up to surface roughness of  $3.316 \mu\text{m}$  and further increase in surface roughness decreased the fatigue and tensile strength of the adhesive bond. SEM images of the specimens indicated that sample 1 showed adhesive type of failure, sample 2 and sample 5 showed fiber failure whereas sample 3 and sample 4 showed mixed type of failure.

### References

1. Kim M-H, Ri J-H, Hong H-S. A 3-D numerical modeling for prediction of mixed failure characteristics in composite single lap joints with hybrid adhesive layer. *Int. J. Adhes. Adhes.* 2022;118: 103223.
2. Lo Presti M, Rizzo G, Farinola GM, Omenetto FG. Bioinspired Biomaterial Composite for All-Water-Based High-Performance Adhesives. *Adv. Sci.* 2021;8(16): 2004786.
3. Yang G, Yang T, Yuan W, Du Y. The influence of surface treatment on the tensile properties of carbon fiber-reinforced epoxy composites-bonded joints. *Compos. Part B Eng.* 2019;160: 446–456.
4. Salimi S, Babra TS, Dines GS, Baskerville SW, Hayes W, Greenland BW. Composite polyurethane adhesives that debond-on-demand by hysteresis heating in an oscillating magnetic field. *Eur. Polym. J.* 2019;121: 109264.
5. Kumar R, Mishra A, Sahoo S, Panda BP, Mohanty S, Nayak SK. Epoxy-based composite adhesives: Effect of hybrid fillers on thermal conductivity, rheology, and lap shear strength. *Polym Adv Technol.* 2019;30(6): 1365–1374.
6. Korayem AH, Li CY, Zhang QH, Zhao XL, Duan WH. Effect of carbon nanotube modified epoxy adhesive on CFRP-to-steel interface. *Compos. Part B Eng.* 2015;79: 95–104.



7. Saraç İ, Adin H, Temiz Ş. Experimental determination of the static and fatigue strength of the adhesive joints bonded by epoxy adhesive including different particles. *Compos. Part B Eng.* 2018;155: 92–103.
8. Van Dam JPB, Abrahami ST, Yilmaz A, Gonzalez-Garcia Y, Terryn H, Mol JMC. Effect of surface roughness and chemistry on the adhesion and durability of a steel-epoxy adhesive interface. *Int. J. Adhes. Adhes.* 2020;96: 102450.
9. Guo L, Liu J, Xia H, Li X, Zhang X, Yang H. Effects of surface treatment and adhesive thickness on the shear strength of precision bonded joints. *Polym. Test.* 2021;94: 107063.
10. Xue G, Zhang B, Sun M, Zhang X, Li J, Wang L, Song C. Morphology, thermal and mechanical properties of epoxy adhesives containing well-dispersed graphene oxide. *Int J Adhes Adhes.* 2019;88: 11–18.
11. Aradhana R, Mohanty S, Nayak SK. Comparison of mechanical, electrical and thermal properties in graphene oxide and reduced graphene oxide filled epoxy nanocomposite adhesives. *Polymer (Guildf).* 2018;141: 109–123.
12. Bansal SA, Singh AP, Kumar S. Reinforcing Graphene Oxide Nanoparticles to Enhance Viscoelastic Performance of Epoxy Nanocomposites. *J. Nanosci. Nanotechnol.* 2019;19(7): 4000–4006.
13. Sammaiah A, Huang W, Wang X. Synthesis of magnetic Fe<sub>3</sub>O<sub>4</sub>/graphene oxide nanocomposites and their tribological properties under magnetic field. *Mater. Res. Express.* 2018;5(10): 105006.
14. Rajaganapathy C, Vasudevan D, Selvakumar N. Investigation on Tribological and mechanical behaviour of AA6082 - Graphene based composites with Ti particles. *Mater. Res. Express.* 2020;7(7): 076514.
15. Banea MD, Da Silva LFM. Adhesively bonded joints in composite materials: An overview. *Proc. Inst. Mech. Eng. Part L J. Mater. Des. Appl.* 2009;223(1): 1–18.
16. Fernández MV, De Moura MFSF, Da Silva LFM, Marques AT. Composite bonded joints under mode I fatigue loading. *Int. J. Adhes. Adhes.* 2011;31(5): 280–285.
17. Wei J, Vo T, Inam F. Epoxy/graphene nanocomposites - processing and properties: a review. *RSC Adv.* 2015;5(90): 73510–73524.
18. Jojibabu P, Zhang YX, Prusty BG. A review of research advances in epoxy-based nanocomposites as adhesive materials. *Int. J. Adhes. Adhes.* 2020;96: 102454.
19. Ghadge RR, Prakash S, Ganorkar SA. Experimental investigations on fatigue life enhancement of composite (e-glass/epoxy) single lap joint with graphene oxide modified adhesive. *Mater. Res. Express.* 2021;8(2): 025202.
20. Budhe S, Ghumatkar A, Birajdar N, Banea MD. Effect of surface roughness using different adherend materials on the adhesive bond strength. *Appl. Adhes. Sci.* 2015;3: 20.
21. Jojibabu P, Zhang YX, Rider AN, Wang J, Wuhner R, Prusty BG. High-performance epoxy-based adhesives modified with functionalized graphene nanoplatelets and triblock copolymers. *Int J Adhes Adhes.* 2020;98: 102521.
22. Upadhyaya P, Kumar S, Reddy JN, Lacy TE. Multiscale modeling of strength and failure behavior of carbon nanostructure reinforced epoxy composite adhesives in bonded systems. *Eur J Mech A/Solids.* 2020;80: 103932.
23. Rafiee MA, Rafiee J, Srivastava I, Wang Z, Song H, Yu ZZ, et al. Fracture and fatigue in graphene nanocomposites. *Small.* 2010;6(2): 179–183.
24. Abdullah SI, Ansari MNM. Mechanical properties of graphene oxide (GO)/epoxy composites. *HBRC J.* 2015;11(2): 151–156.
25. Soltannia B, Taheri F. Influence of nano-reinforcement on the mechanical behavior of adhesively bonded single-lap joints subjected to static, quasi-static, and impact loading. *J. Adhes Sci Technol.* 2015;29(5): 424–442.

26. Shokrieh MM, Esmkhani M, Haghghatkah AR, Zhao Z. Flexural fatigue behavior of synthesized graphene/carbon-nanofiber/epoxy hybrid nanocomposites. *Mater Des.* 2014;62: 401–408.
27. Kiran BV, Rao KM, Raju DL. An investigation on mechanical properties of e-glass fiber reinforced polymer nanocomposites. *Mater Today Proc.* 2019;18: 5454–5463.
28. Bortz DR, Heras EG, Martin-Gullon I. Impressive fatigue life and fracture toughness improvements in graphene oxide/epoxy composites. *Macromolecules.* 2012;45(1): 238–245.
29. Jahandideh S, Shirazi MJS, Tavakoli M. Mechanical and thermal properties of octadecylamine-functionalized graphene oxide reinforced epoxy nanocomposites. *Fibers Polym.* 2017;18(10): 1995–2004.

## THE AUTHORS

**Manoli Ashutosh** 

e-mail: ashul6manoli@gmail.com

**Rohit Ghadge** 

e-mail: rohit.ghadge@mitwpu.edu.in

**Parshant Kumar** 

e-mail: parshant.kumar@mitwpu.edu.in